



2024, MILANO

Unveiling Advanced Frequency Disentanglement Paradigm for Low-Light Image Enhancement

Kun Zhou* , Xinyu Lin* , Wenbo Li , Xiaogang Xu, Yuanhao Cai,
Zhonghang Liu ,Xiaoguang Han , and Jiangbo Lu✉



香港中文大學(深圳)

The Chinese University of Hong Kong, Shenzhen



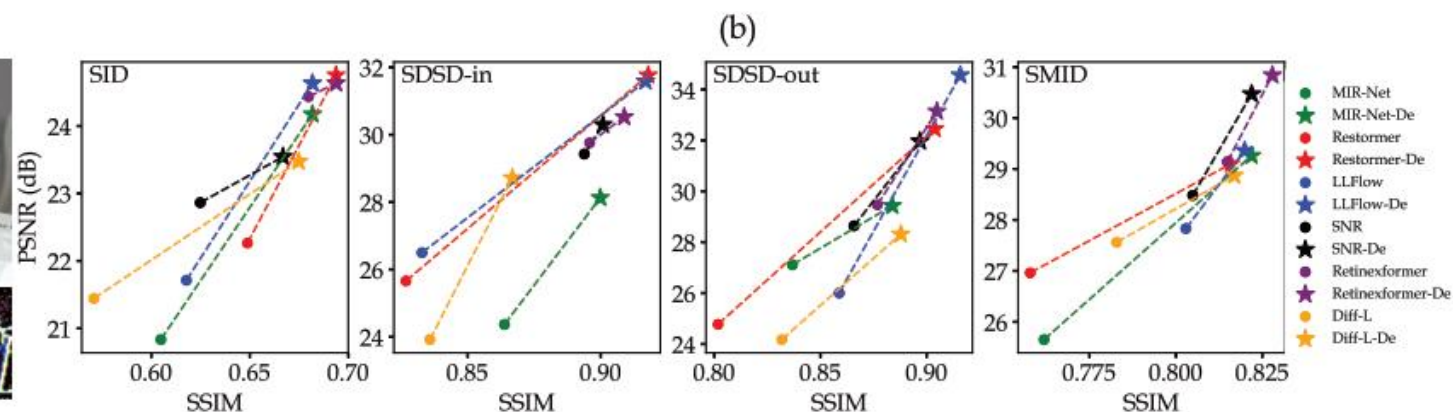
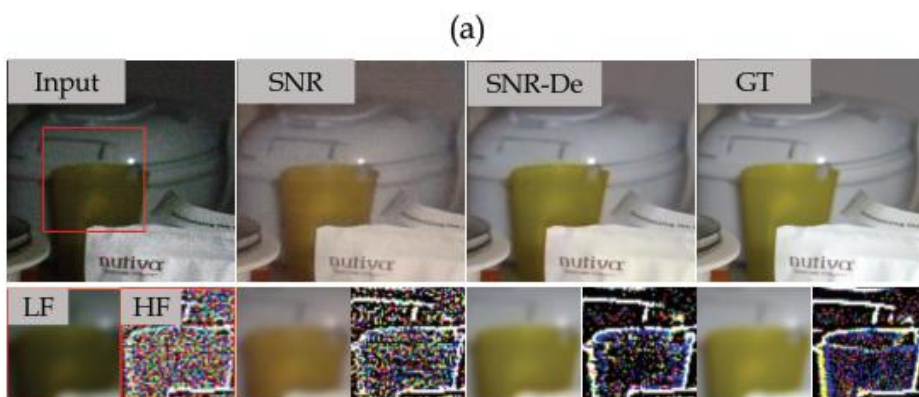
JOHNS HOPKINS
UNIVERSITY



SMU
SINGAPORE MANAGEMENT
UNIVERSITY

Motivation

- **Background.** Existing methods for Low-Light Image Enhancement face significant challenges in optimizing combined low- and high-frequency restoration within a unified framework.
- **Issues to be solved.**
 - Seamlessly integrating with existing LLIE methods
 - Enhancing their frequency restoration capabilities (up to +7.9dB improvements)
 - Requiring a minimal additional model complexity (~88K extra parameters)



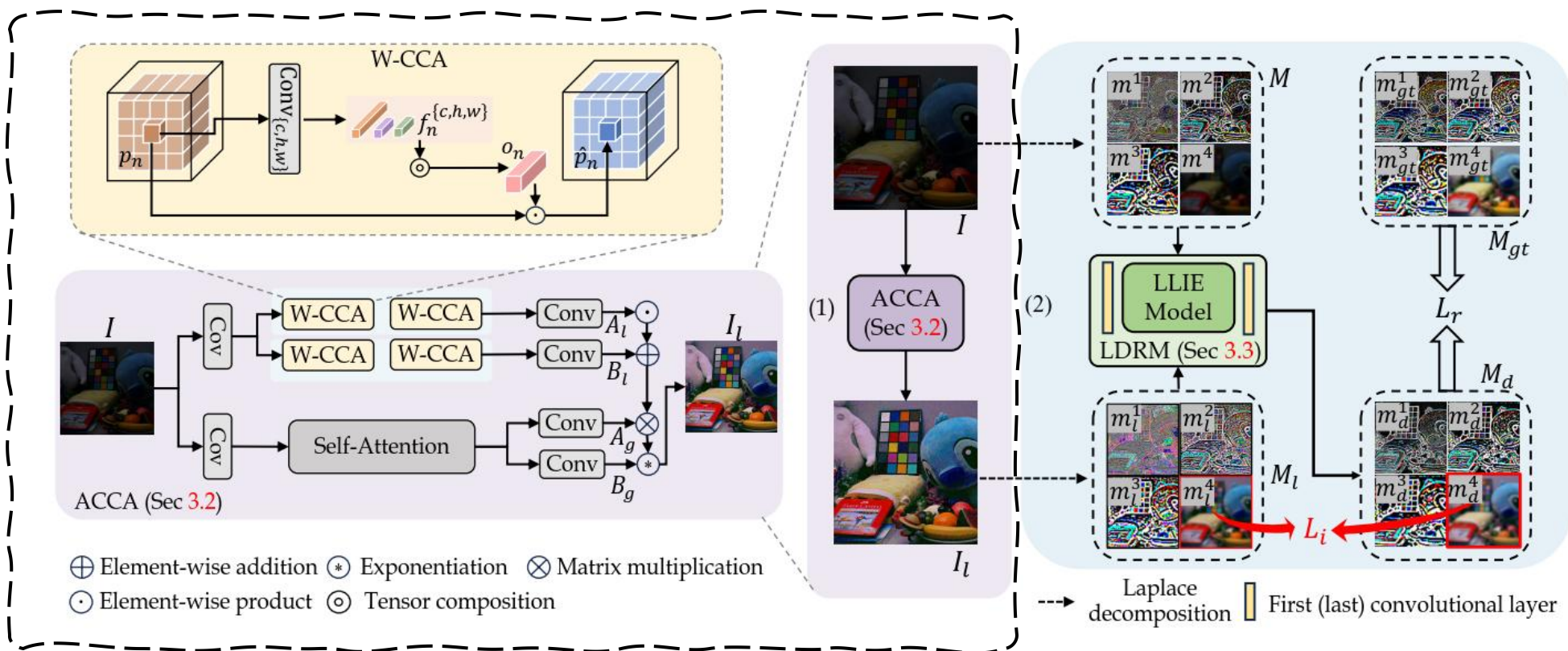
Contribution



Our contributions are summarized:

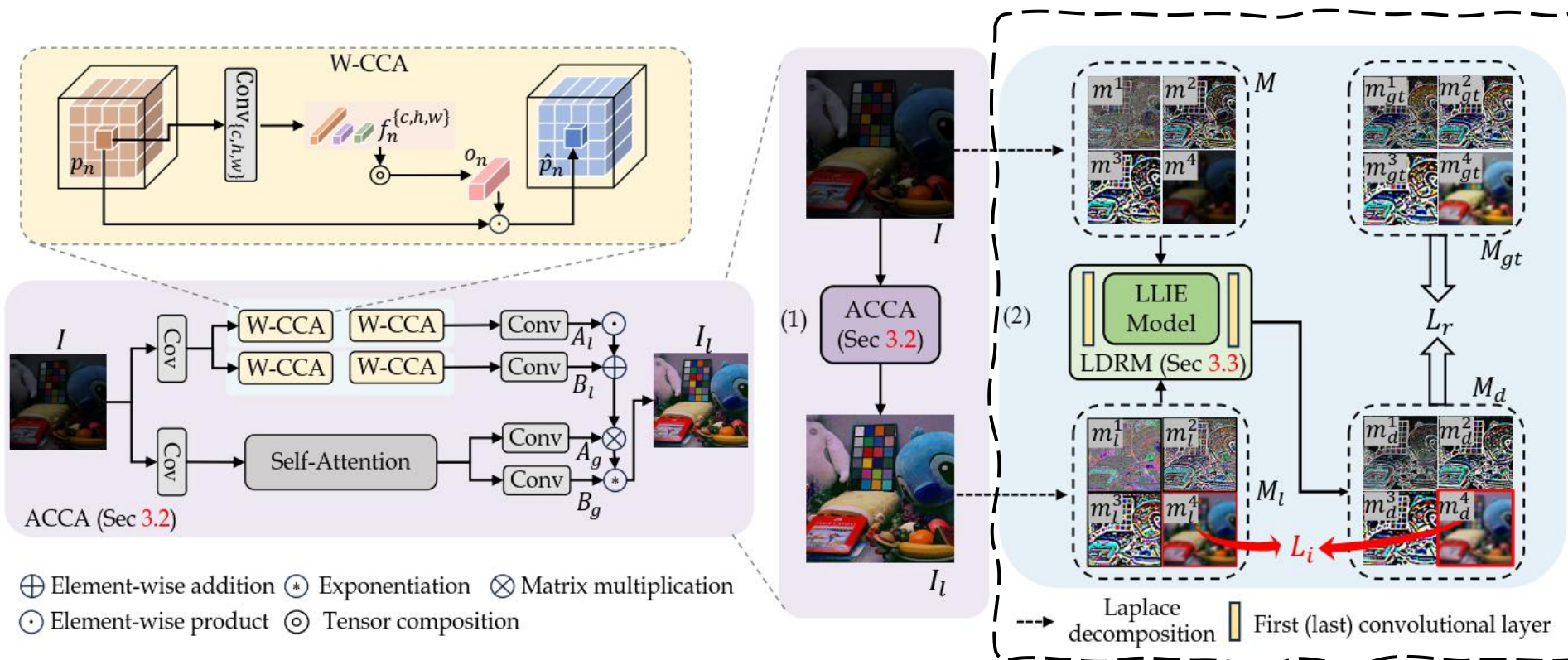
- **Disentanglement learning.** *This strategy achieves separate optimization in the low-frequency and high-frequency domains while maintaining low-frequency consistency between the two stages.*
- **Efficient coarse adjustment.** *ACCA, a extreme lightweight module implement convolutional adaptive spatial-channel aggregation, resulting in SOTA low-frequency adjustment results.*
- **Universal improvements over SOTA models.** *It allows effortless deployment of advanced low-frequency or high-frequency enhancement models. Leveraging our method, we significantly improve prevailing LLIE models both quantitatively and qualitatively.*

Overview



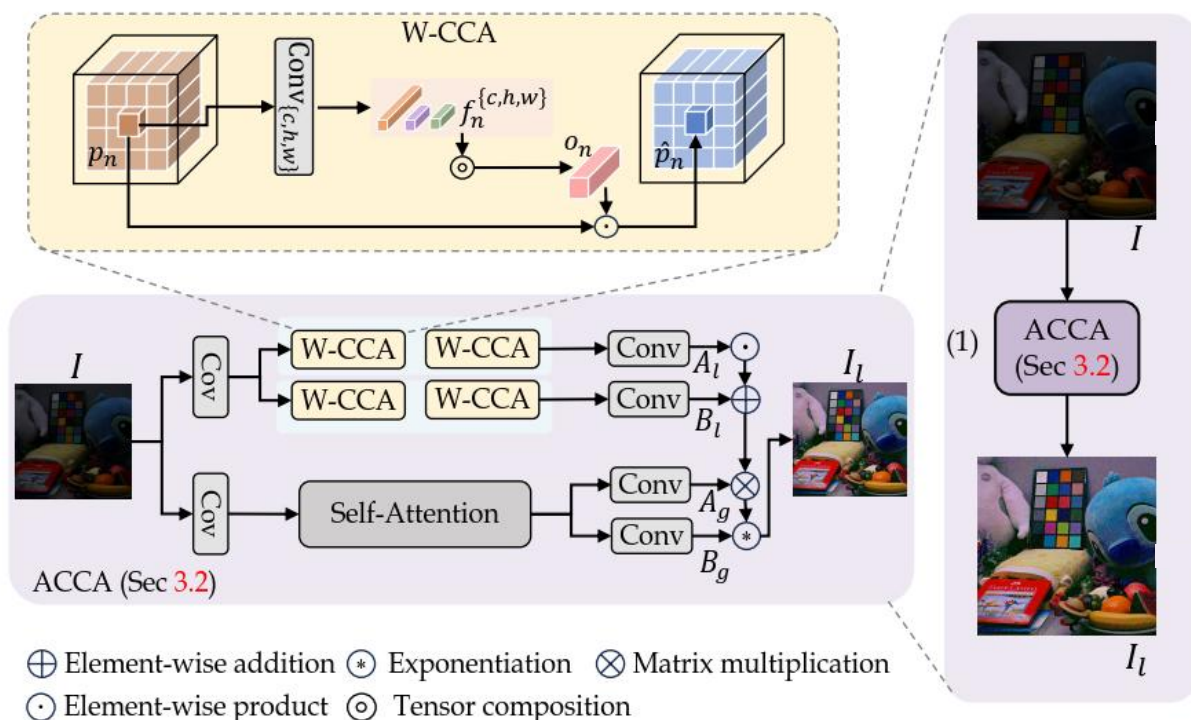
- **Coarse phase.** ACCA conducts coarse adjustment to initially enhance the input image I and produce the preliminary result I_l .

Overview



- **Coarse-to-fine phase.** LDRM integrates Laplace representations for subsequent fine-grained restoration by LLIE model. Low-frequency consistent loss L_i between the two phases is introduced to achieve effective disentanglement optimization.

ACCA for Coarse Adjustment



- Overview: hybrid dual-branch network to regress global and local low-frequency adjustment parameters.

$$I_l^{local} = A_l \odot I \oplus B_l, \quad I_l = (A_g \otimes I_l^{local})^{B_g}$$

- W-CCA: novel window-based convolutional composition method with significant reduction in computational complexity.

$$\hat{p}_n = o_n \odot p_n$$

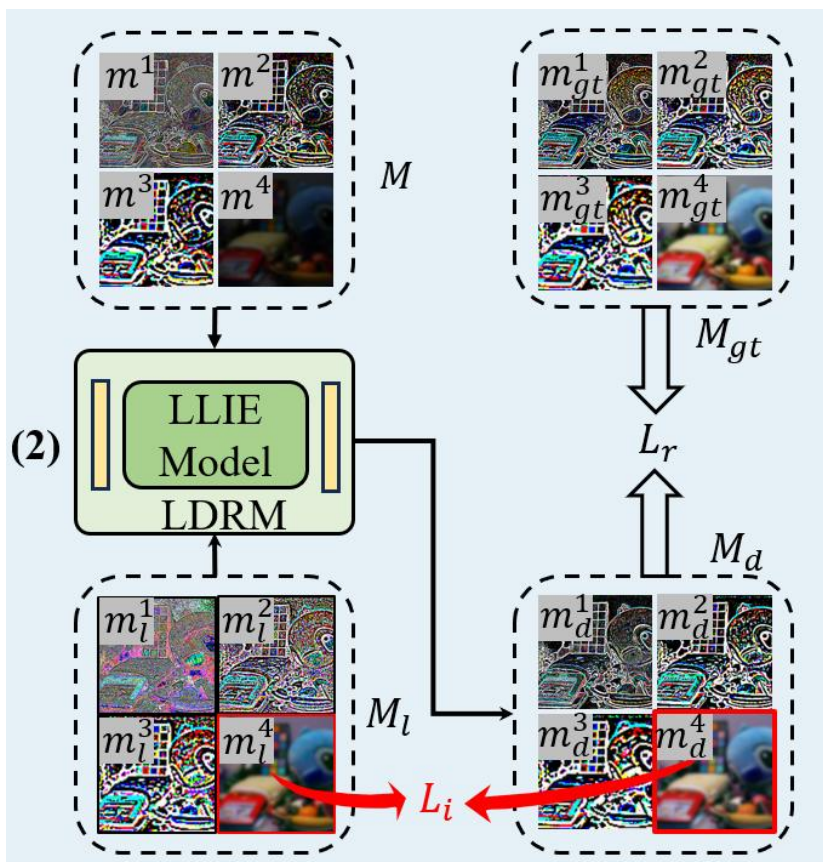
$$o_n = f_n^h \odot f_n^w \odot f_n^c$$

$$f_n^{\{h,w,c\}} = \text{Conv}_{\{h,w,c\}}(p_n, s, s).$$

- Complexity analysis of W-CCA.

$$\mathcal{O}(\text{W-CCA}) = 4HWC + 2HWC^2/s.$$

LDRM for Consistent C2F Restoration



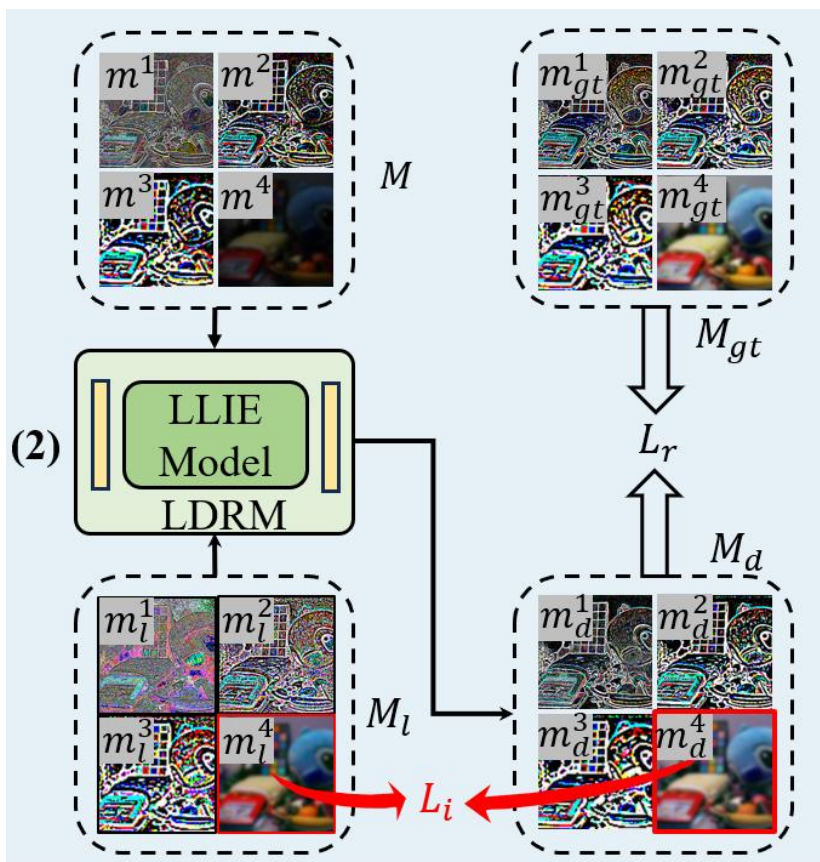
- We re-design SOTA existing LLIE models by integrating Laplace representation and obtain Laplace maps:

$$m^k = \begin{cases} I - I_G^k; & \text{if } k = 1 \\ \text{resize}(I_G^{k-1}, \downarrow 2) - I_G^k; & \text{if } K > k > 1 \\ \text{resize}(I_G^{k-1}, \downarrow 2); & \text{if } k = K \end{cases}$$

- All these decomposed Laplace maps are fed into our LDRM to generate restored Laplace maps.
- The final reconstructed output is obtained by inverse Laplace transformation:

$$\hat{m}^k = \begin{cases} m^K; & \text{if } k = K \\ m^k + \text{resize}(m^{k+1}, \uparrow 2); & \text{otherwise} \end{cases}$$

LDRM for Consistent C2F Restoration



- Training LDRM, we use two supervision terms:

- Reconstruction Loss

$$L_r = \sum_{i=1}^K (\|m_d^i - m_{gt}^i\|_1)$$

- Low-frequency Loss

$$L_i = \|m_d^K - m_l^K\|_1$$

- Total Loss

$$L_{total} = L_r + \alpha * L_i$$

Quantitative Comparison

Table 1: Quantitative results (PSNR (dB)/SSIM) on five challenging LLIE benchmarks. ‘-De’ refers to the enhanced version of our proposed approach and ‘Improve.’ refers to the improvements attained by our method compared to the six baselines.

Method	LOL-v2	SID	SDSD-in	SDSD-out	SMID
	PSNR/SSIM	PSNR/SSIM	PSNR/SSIM	PSNR/SSIM	PSNR/SSIM
MIR-Net [56]	20.02/0.820	20.84/0.605	24.38/0.864	27.13/0.837	25.66/0.762
MIR-Net-De	24.19/0.882	24.18/0.682	28.14/0.900	29.45/0.884	29.27/0.822
Improve.	+4.17/+0.062	+3.34/+0.075	+3.76/+0.036	+2.32/+0.047	+1.16/+0.072
Restormer [55]	19.94/0.827	22.27/0.649	25.67/0.827	24.79/0.802	26.97/0.758
Restormer-De	24.56/0.893	24.76/0.694	31.78/0.918	32.47/0.904	29.11 /0.816
Improve.	+4.62/+0.066	+2.49/+0.045	+6.11/+0.091	+7.68/+0.102	+2.14/+0.058
LLFlow [45]	26.20/0.888	21.72/0.618	26.51/0.883	26.02/0.859	27.84/0.803
LLFlow-De	28.90/0.908	24.64/0.682	31.60/0.917	34.58/0.916	29.37/0.820
Improve.	+1.70/+0.020	+2.92/+0.064	+5.09/+0.034	+8.83/+0.057	+1.53/+0.017
SNR [51]	21.48/0.849	22.87/0.625	29.44/0.894	28.66/0.866	28.49/0.805
SNR-De	24.00/0.872	23.55/0.667	30.31/0.901	31.98/0.897	30.48/0.822
Improve.	+2.52/+0.023	+0.68/+0.042	+0.87/+0.007	+3.32/+0.031	+1.99/+0.017
Retinexformer [3]	22.80/0.840	24.44/0.680	29.77/0.896	29.49/0.877	29.15/0.815
Retinexformer-De	24.21/0.881	24.64/0.694	30.54/0.909	33.16/0.905	30.85 /0.828
Improve.	+1.41/+0.041	+0.20/+0.014	+0.77/+0.013	+3.67/+0.028	+1.70/+0.013
Diff-L [15]	18.95/0.722	21.45/0.571	23.93/0.836	24.19/0.832	27.57/0.783
Diff-L-De	23.93/0.853	23.48/0.675	28.73/0.867	28.33/0.888	28.88/0.817
Improve.	+4.98/+0.081	+2.03/+0.104	+4.80/+0.031	+4.14/+0.056	+1.31/+0.034

Quantitative Comparison : ACCA

Table 4: Quantitative comparison between ACCA and other SOTA LLIE models on LOL-v2 [52] benchmark. The best and second-best results are highlighted in **red** and **blue**, respectively. We test the inference speed (FPS: Frames Per Second) with an input size of 256×256 on an NVIDIA RTX 3090 GPU.

Method	Venue	PSNR \uparrow	SSIM \uparrow	Params. \downarrow	FPS \uparrow
ZeroDCE [11]	CVPR 2020	17.63	0.617	0.079M	62.50
Star [58]	ICCV 2021	18.26	0.546	0.027M	58.82
IAT [6]	BMVC 2022	23.50	0.824	0.091M	45.45
PairLIE [9]	CVPR 2023	18.80	0.721	0.342M	55.56
ACCA (Ours)	ECCV 2024	23.80	0.829	0.088M	125
MIR-Net [56]	ECCV 2020	20.02	0.820	31.79M	4.87
MIR-Net-v2 [57]	T-PAMI 2022	21.10	0.821	5.86M	15.6
Restormer [55]	CVPR 2022	19.94	0.827	26.13M	9.62
SNR [51]	CVPR 2022	21.48	0.849	39.12M	83.33
Retinexformer [3]	ICCV 2023	22.80	0.840	1.61M	27.03
LLformer [44]	AAAI 2023	20.69	0.759	24.55M	8.85
Diff-L [15]	Sig. Asia 2023	18.96	0.723	22.08M	4.41

Quantitative Comparison

Table 2: We present comprehensive details regarding model complexities, including parameters, GFLOPS, and inference time. Consistent with [3], we assess GFLOPS and inference time using an input size of 256×256 , utilizing an NVIDIA-RTX 3090 GPU. It's worth highlighting that our framework (denoted as 'w/ ours') entails only 0.2%-5.5% additional parameters for enhancing the state-of-the-art LLIE models.

Methods	MIR-Net	Restormer	LLFlow	SNR	Retinexformer	Diff-L	w/ ours
Param.(M)	31.79	26.13	37.68	39.12	1.61	22.08	+0.088
GFLOPS	785	144.25	287	26.35	15.57	88.92	+2.53
Speed(s)	0.205	0.104	0.267	0.039	0.079	0.227	+0.008

Qualitative Comparison

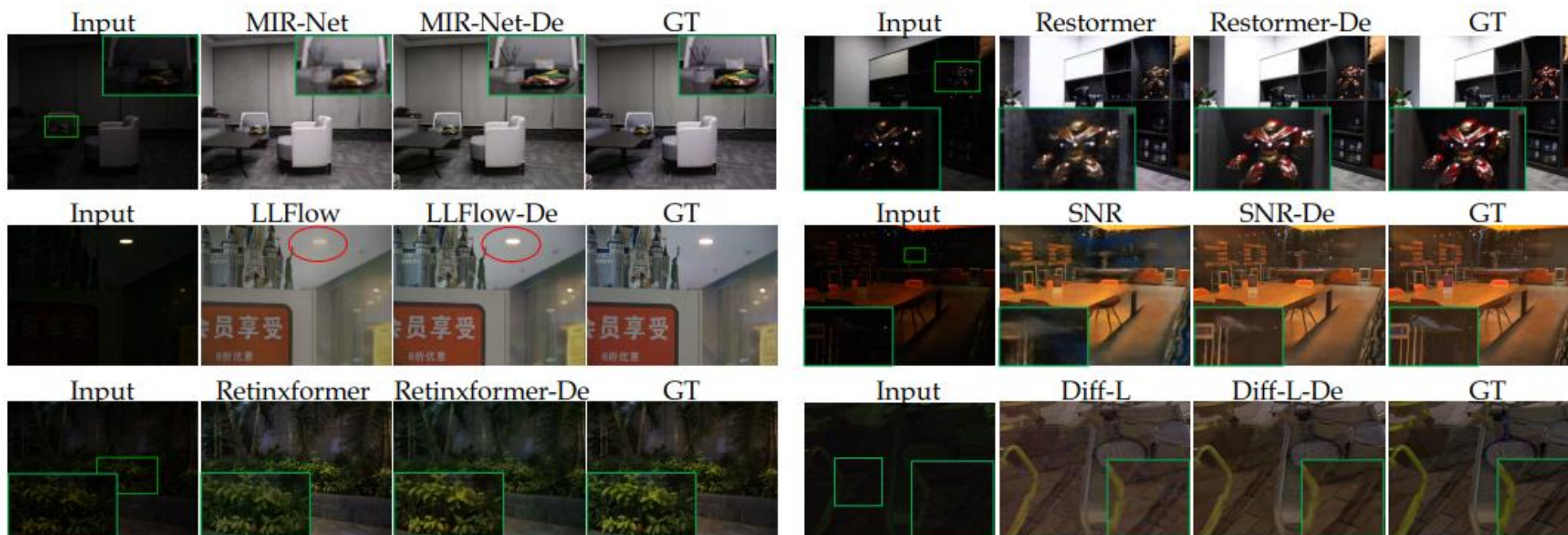


Fig. 3: Qualitative evaluation on several benchmarks. Our integration provides accurate outcomes for both high-frequency (clearer image detail restoration) and low-frequency (more accurate illumination recovery) areas.

Ablation Studies

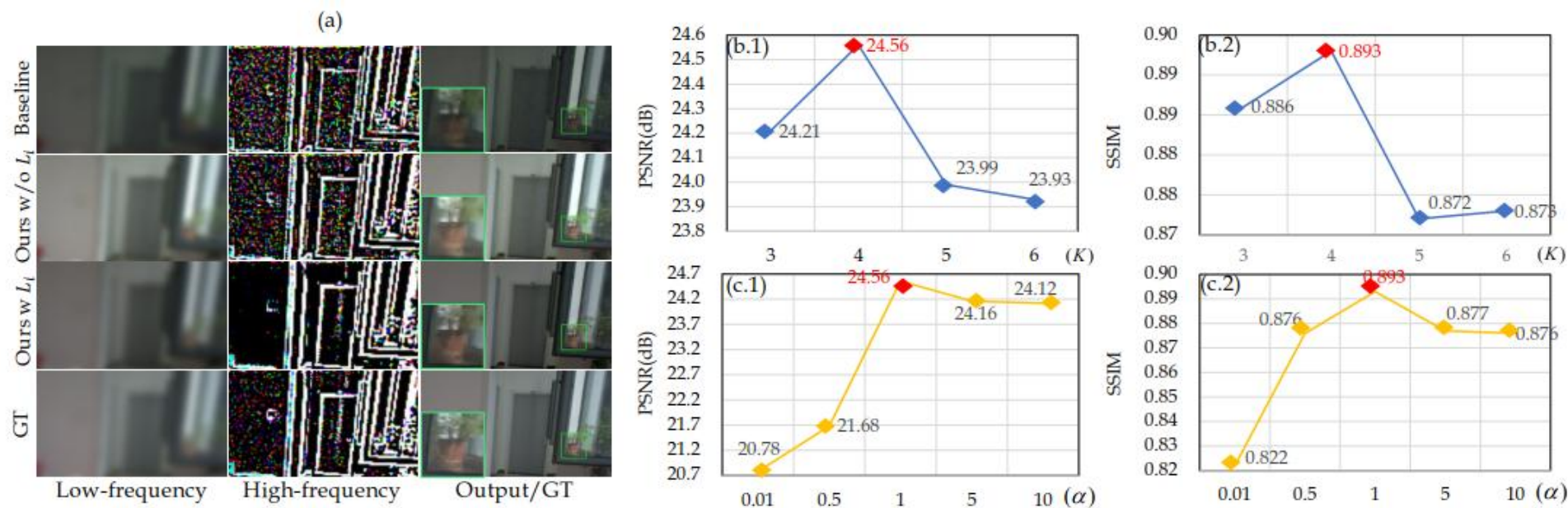


Fig. 4: (a) Visual validation of our disentanglement learning. (b-c) Impact of adopting different settings in our method: (b.1-2) different pyramid levels (K) in Laplace representation; (c.1-2) different α values to conduct low-frequency consistent supervision.

Ablation Studies

Table 6: Effectiveness of our ACCA and L_i .

Model	Restormer	ACCA	L_i	PSNR/SSIM	Param./FLOPS
Baseline	✓			19.94/0.827	26.13M/144.25G
Ours w/o L_i	✓	✓		20.21/0.837	26.22M/146.78G
Ours w/ L_i	✓	✓	✓	24.56/0.893	26.22M/146.78G

Table 7: Quantitative comparison between two different optimization schemes.

Baseline	Retinexformer	Restormer	MIRNet	SNR	LLFlow	Diff-L
End-to-end	24.13/0.878	24.27/0.885	24.05/0.880	23.82/0.864	27.94/0.896	23.90/0.847
Ours	24.21/0.881	24.56/0.893	24.19/0.882	24.00/0.872	28.90/0.908	23.93/0.853



2024, MILANO

Thank You

Unveiling Advanced Frequency Disentanglement Paradigm for Low-Light Image Enhancement



香港中文大學(深圳)

The Chinese University of Hong Kong, Shenzhen

